Kinetostatic Analysis of a Simple Cable-Driven Parallel Crane

Saman Lessanibahri, Philippe Cardou, Stéphane Caro

Proceedings of the ASME 2018 International Design Engineering Technical Conferences & Computers and Information in Engineering Conference
IDETC/CIE 2018
August 26-29, 2018, Quebec City, Canada

DETC2018-86173

KINETOSTATIC ANALYSIS OF A SIMPLE CABLE-DRIVEN PARALLEL CRANE

Saman Lessanibahri[1,2], Philippe Cardou[3], Stéphane Caro[2,4]*
[1] École Centrale de Nantes, Nantes, 44321 France
[2] Laboratoire des Sciences du Numérique de Nantes (LS2N), UMR CNRS 6004, Nantes, 44300, France
[3] Laboratoire de robotique, Département de génie mécanique, Université Laval, Québec, QC, Canada
[4] Centre National de la Recherche Scientifique (CNRS), Nantes, 44321, France
Emails: Saman.Lessanibahri@ls2n.fr
Philippe.Cardou@gmc.ulaval.ca, Stephane.Caro@ls2n.fr

ABSTRACT

This paper introduces the concept of a new planar Cable-Driven Parallel Crane (CDPC) for lifting and carrying payloads with a moving hoist mechanism connected in parallel to the ceiling. In contrast to bridge-crane, CDPC is inexpensive and practicable for diverse tasks with simple assembly setup. The hoist mechanism is an under-constrained moving-platform articulated through a bi-actuated cable circuit, namely, a cable loop. The hoist is connected to a suspended moving-platform with four degrees of freedom. The power is transmitted directly from the motors fixed on frames to the hoist through the cable loop. Therefore, the dynamic performance of the robot is increased due to lower inertia of the moving-platform. However, the moving-platform undergoes some parasitic inclinations because of the cable loop. This paper investigates the parasitic inclination and its effect on the positioning of the payload. The workspace of the CDPC is studied in terms of static equilibrium. Moreover, the geometrico-static and elasto-static models of the CDPC are presented.

1 INTRODUCTION

Nowadays, overhead cranes or bridge-cranes are widely used in the industry. They usually consist in runways fixed to a ceiling which accommodates a hoist mechanism for lifting or lowering payloads. They are applicable for heavy-payload tasks. However, the bridge-cranes have some drawbacks that reduce their utilization, i.e., they are bulky, expensive and should adapt to the structure of the buildings.

On the other hand, Cable-Driven Parallel Robots (CDPRs) may seem a sound alternative for the bridge cranes as it can overcome the above-mentioned issues. A CDPR consists of a base frame, a Moving-Platform (MP) and a set of cables connecting in parallel the MP to the base frame. CDPRs have some advantages over bridge cranes. Indeed, they are easy to reconfigure [1], easy to assemble and comparatively inexpensive. Nevertheless, they suffer from cable interferences with surrounding environment.

In this paper, we introduce the concept of a planar under-constrained Cable-Driven Parallel Crane (CDPC) that is able to lift and lower payloads throughout its workspace. The idea is to combine the advantageous features of CDPRs with bridge cranes as shown in Fig. 1. The CDPC is a CDPR with a hoist connected to its MP. This design enables us to improve CDPR capabilities for carrying payloads while eliminating their issue regarding interference between cables and objects on the ground. The concept of attaching the hoist to the MP is applicable as long as the hoist mechanism does not require motorization on the MP. Motorization on the MP leads to lower-level dynamic performance due to the higher inertia and interference between motor wires and cables of the CDPR. We could overcome this issue by employing a cable loop. A cable loop is a cable forming a closed circuit actuated by two motors. The cable loop enables us to design an articulated platform without having a motor on the MP.

*Address all correspondence to this author.

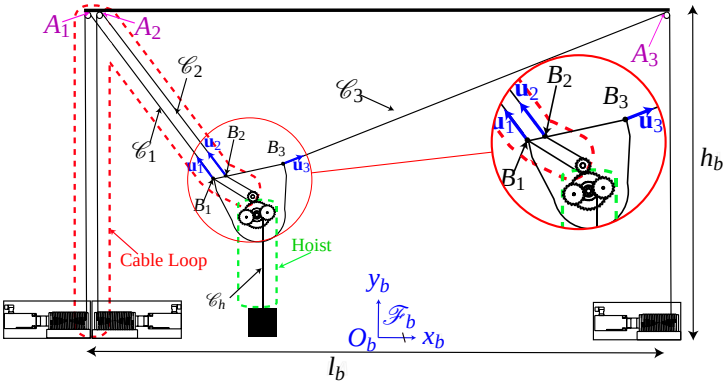

Figure 1: A FOUR-DoF PLANAR CABLE-DRIVEN PARALLEL ROBOT WITH A CABLE LOOP

The hoist is driven by a drum that is connected to the cable loop and actuates a cable, which lifts or descends a payload by wrapping around a drum. The proposed hoist mechanism consists in a triple-stage gear reducer that increases the output torque by 10 times.

The paper is organized into six sections. Section 2 describes the conceptual design model of a CDPC with an under-constrained hoist as the MP. The geometrico-static and elasto-static models of the CDPC are presented in Sec. 3. Section 4 studies the minimum required height of the CDPC for manipulating a given payload. In addition, this section deals with the workspace analysis of the robot depending on the minimum required height, payload weight and motors torque. Section 5 details the effect of the hoisting torque on the positioning of the payload. The positioning accuracy depends on the parasitic inclinations originated from the cable loop. Finally, conclusions are drawn and future works are presented in Section 6.

2 MANIPULATOR ARCHITECTURE

Here, we discuss the architecture of the CDPC. The overall manipulator consists in a base frame and a MP connected in parallel by two actuated cables as shown in Fig. 1. The under-actuated MP possesses four Degree of Freedom (DoF) within a planar workspace. The MP has two translational DoF in the **x***O***y** plane, one rotational DoF of axis normal to its translation plane. The actuation of the additional degree of freedom on the MP is done through a cable loop and a drum, so that no motor needs to be mounted on the MP for actuation of the end-effector.

The proposed manipulator consists in an articulated MP actuated by three motors through two cables. The MP accommodates a hoist mechanism, which is coupled with a cable loop. The cable loop has two distinct purposes. The former is devoted to the positioning of the MP and the latter is reserved for the actuation of the hoist. The hoist consists in a triple-stage reducer that increases the input torque generated by the cable loop and transmits it to a cable, $\mathscr{C}_h$, that is wound onto a drum. Therefore, The relative height between the given payload and the MP can be adjusted within the workspace of the CDPC. As the proposed application of the CDPC does not require its MP to approach the payload, the risk of collision between objects on the ground with cables of the robot is eliminated.

Figure 2 illustrates the overall schematic of the MP of the CDPC. The MP is suspended by two cables, i.e., a cable loop ($\mathscr{C}_1$ and $\mathscr{C}_2$) that are actuated by two motors and another cable, $\mathscr{C}_3$, that connects the support of the MP to the third motor. The cables are directly connected to the support of the MP and the hoist mechanism is accommodated within the support. The hoist is outlined in the figure and its main task is to transmit the power from input shaft, $\mathscr{S}_1$, to the second shaft, $\mathscr{S}_2$. The input shaft is actuated by two motors fixed to the ground and through the cable loop. The gear train inspired from the one in [1] increases the input torque and transfer it to $\mathscr{S}_2$. The second shaft, transmits the power to the hoist drum, $\mathscr{D}_h$, through the gear train. Consequently, $\mathscr{C}_h$, is wound onto $\mathscr{D}_h$. However, $\mathscr{S}_2$ and $\mathscr{D}_h$ are concentric, they are not in contact.

The cable loop connected to two actuators, which are shown in Fig. 1, is coiled about $\mathscr{D}_p$ to make the latter rotate about its own axis. The left side of this cable loop is denoted by $\mathscr{C}_1$ whereas its right side is denoted by $\mathscr{C}_2$. Another cable, identified by $\mathscr{C}_3$, is connected to both the support of the articulated MP and a third actuator. The cable loop consists in two segments each with independent cable tensions t_1 and t_2. Segment $\mathscr{C}_1$, is composed of the part of the cable loop, which connects the first motor to the drum through points A_1 and B_1. The second segment is denoted as $\mathscr{C}_2$ and connects the second motor to the drum through points A_2 and B_2. Two motions can be induced by the cable loop depending on the relative rotation of two actuators connected to the cable loops. First one is the displacement of point C (the center of $\mathscr{D}_p$ shown in Fig. 3) for identical inputs to the two motors. And the second motion is a rotation about point C when the two actuators rotate in opposite directions.

Figure 3 shows the geometry of the MP of the CDPC. The MP frame, $\mathscr{F}_p$, is located on the top of MP and belongs to the vertical center-line of the MP, $\mathscr{L}_v$. The overall dimension of the MP is specified by h_p and l_p that denote the height and length of the MP, respectively. The radius of $\mathscr{D}_p$ is denoted as r_p. Anchor points B_1 and B_3 are located on the top corners of the MP, so that the length of the MP is computed as $l_p = b_{3x} - b_{1x}$.

3 STATIC MODEL OF CABLE-DRIVEN PARALLEL CRANE

This section studies the mathematical modeling of the under-constrained CDPC shown in Fig. 1. The geometric model

[1] https://youtu.be/ZA0izXvmzMg

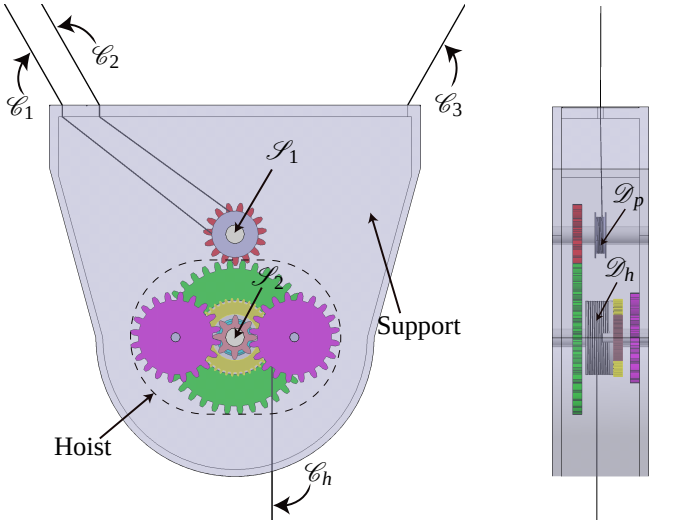

(a) Front view (b) Side view

Figure 2: MOVING-PLATFORM OF CABLE-DRIVEN PARALLEL CRANE

alongside static equilibrium equations are presented. Following the latter models, elasto-static model and accordingly, the stiffness matrix of the MP are presented.

Geometrico-static model of the CDPC

Loop-closure equations of the CDPC are given by

$$ {}^b\mathbf{l}_i = {}^b\mathbf{a}_i - {}^b\mathbf{p} - {}^b\mathbf{R}_p {}^p\mathbf{b}_i, \quad i = 1,\ 2,\ 3 \tag{1} $$

where ${}^b\mathbf{l}_i$ is the ith cable vector, i.e., the Cartesian coordinate vectors pointing from point B_i to point A_i. Points A_i and B_i stand for the ith cable exit point and anchor point, respectively. The former point is the location of ith pulley fixed to the ceiling and the latter is the connection point between the cable and the MP. ${}^b\mathbf{a}_i = [a_{ix},\ a_{iy}]^T$, ${}^p\mathbf{b}_i = [b_{ix},\ b_{iy}]^T$ and ${}^b\mathbf{p} = [p_x,\ p_y]^T$ are the Cartesian coordinate vector of points A_i, B_i and P, respectively. ${}^b\mathbf{R}_p$ is the rotation matrix from frame $\mathscr{F}_b$ to frame $\mathscr{F}_p$ and is expressed as follows:

$$ {}^b\mathbf{R}_p = \begin{bmatrix} \cos\theta & -\sin\theta \\ \sin\theta & \cos\theta \end{bmatrix} \tag{2} $$

$\theta = \angle(\mathbf{x}_b,\ \mathbf{x}_p)$ is the rotation angle of the MP. $\mathbf{t}_i,\ i = 1,\ 2,\ 3$ is the ith cable tension vector and it is directed from B_i toward the exit point A_i. $\mathbf{t}_i = t_i {}^b\mathbf{u}_i$ and its magnitude is expressed as $t_i = \|\mathbf{t}_i\|_2$, $i = 1,\ 2,\ 3$ and ${}^b\mathbf{u}_i$ is denoted as the ith cable unit vector. In

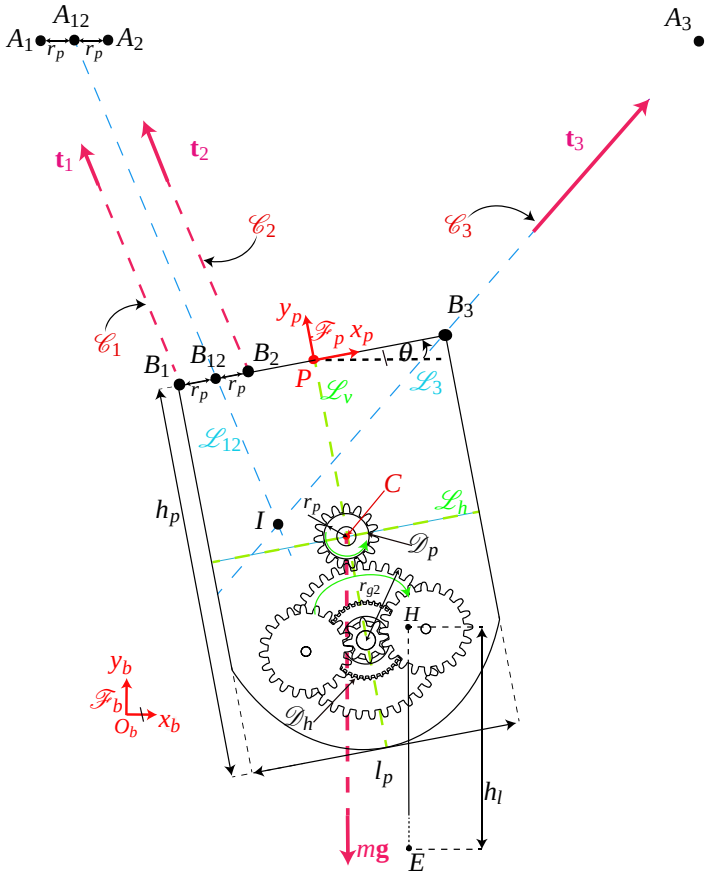

Figure 3: MOVING-PLATFORM OF THE FOUR-DoF PLANAR UNDER-CONSTRAINED CABLE-DRIVEN PARALLEL ROBOT

order to compute the unit cable vector, ${}^b\mathbf{u}_i$, we normalize, ${}^b\mathbf{l}_i$ as follows:

$$ \mathbf{u}_i = \frac{\mathbf{l}_i}{l_i}, \quad i = 1,\ 2,\ 3 \tag{3} $$

l_i being the ith cable length. The external wrenches exerted on the MP are cable tensions, $\mathbf{t}_i,\ i = 1,\ 2,\ 3$, the weight of the MP, $m\mathbf{g}$, and the frictional moment or the resistance to relative motions between $\mathscr{D}_p$ and the hoist that is denoted as m_{fr}. The equilibrium of the external forces applied onto the MP, is expressed as follows:

$$ \sum_{i=1}^{3} t_i {}^b\mathbf{u}_i + m\mathbf{g} = 0 \tag{4} $$

In Eq. (4), m is the mass of the MP and $\mathbf{g} = [0,\ -g]^T$ is the gravity

acceleration with $g = 9.81\ m.s^{-2}$. The equilibrium of moments about point P in frame $\mathscr{F}_b$ is expressed as follows:

$$\sum_{i=1}^{3}\left(\left({}^b\mathbf{b}_i - {}^b\mathbf{p}\right)^T \mathbf{E}^T \mathbf{t}_i\right) + \left({}^b\mathbf{c} - {}^b\mathbf{p}\right)^T \mathbf{E}^T m\mathbf{g} = 0 \tag{5}$$

${}^b\mathbf{c}$ being the Cartesian coordinate vector of the MP Center of Mass (CoM) in $\mathscr{F}_b$, which is expressed as follows:

$${}^b\mathbf{c} = {}^b\mathbf{p} + {}^b\mathbf{R}_p\, {}^p\mathbf{c} \tag{6}$$

${}^p\mathbf{c} = [c_x,\ c_y]^T$ is the Cartesian coordinate vector of the CoM expressed in $\mathscr{F}_p$.
By considering $({}^b\mathbf{b}_i - {}^b\mathbf{p}) = {}^b\mathbf{R}_p\, {}^p\mathbf{b}_i$, $i = 1,\ 2,\ 3$, and $({}^b\mathbf{c} - {}^b\mathbf{p}) = {}^b\mathbf{R}_p\, {}^p\mathbf{c}$ we can rewrite Eq. (5) as follows:

$$\sum_{i=1}^{3}\left({}^p\mathbf{b}_i^T\, {}^b\mathbf{R}_p^T \mathbf{E}^T \mathbf{t}_i\right) + {}^p\mathbf{c}^T\, {}^b\mathbf{R}_p^T \mathbf{E}^T m\mathbf{g} = 0 \tag{7}$$

Finally, we write the equilibrium of the moments generated by cable loop about point P, the latter is the moment that drives $\mathscr{D}_p$ and consequently actuates $\mathscr{D}_h$ and it is formulated as follows:

$$r_p \delta t + m_{fr} = 0 \tag{8}$$

The cable loop tension difference is expressed in the following:

$$\delta t = t_2 - t_1 \tag{9}$$

From Eqs. (4), (7) and (8), the static equilibrium equation of the MP is expressed as:

$$\mathbf{W}\mathbf{t} + \mathbf{w}_e = \mathbf{0}_4 \tag{10}$$

where $\mathbf{W}$ is the wrench matrix of the CDPC under study

$$\mathbf{W} = \begin{bmatrix} {}^b\mathbf{u}_1 & {}^b\mathbf{u}_2 & {}^b\mathbf{u}_3 \\ {}^p\mathbf{b}_1^T\, {}^b\mathbf{R}_p^T \mathbf{E}^T\, {}^b\mathbf{u}_1 & {}^p\mathbf{b}_2^T\, {}^b\mathbf{R}_p^T \mathbf{E}^T\, {}^b\mathbf{u}_2 & {}^p\mathbf{b}_3^T\, {}^b\mathbf{R}_p^T \mathbf{E}^T\, {}^b\mathbf{u}_3 \\ -r_p & r_p & 0 \end{bmatrix} \tag{11}$$

$\mathbf{w}_e$ is the external wrench applied onto the MP

$$\mathbf{w}_e = [0 \quad -mg \quad {}^p\mathbf{c}^T\, {}^b\mathbf{R}_p^T \mathbf{E}^T m\mathbf{g} \quad m_{fr}]^T \tag{12}$$

$\mathbf{0}_4$ is a four dimensional zero vector and the three-dimensional cable tension vector $\mathbf{t}$ is expressed as follows:

$$\mathbf{t} = [t_1 \ \ t_2 \ \ t_3]^T \tag{13}$$

Elasto-static model of CDPC

In order to study the stiffness, the elasto-static model of the MP is given by

$$\delta\mathbf{w}_e = \begin{bmatrix} \delta\mathbf{f}_p \\ \delta m_p \\ \delta m_d \end{bmatrix} = \mathbf{K}\delta\mathbf{r} = \mathbf{K}\begin{bmatrix} \delta\mathbf{p} \\ \delta o_p \\ \delta o_d \end{bmatrix} \tag{14}$$

In Equation (14), $\delta\mathbf{w}_e$ is denoted as the infinitesimal change in the external wrench. $\mathbf{K}$ and $\delta\mathbf{r}$ stand for the stiffness matrix and infinitesimal screw of the MP. The vectors of infinitesimal change in the force and displacement are denoted as $\delta\mathbf{f}_p = [\delta f_x, \delta f_y]^T$ and $\delta\mathbf{p} = [\delta p_x, \delta p_y]^T$, respectively. δm_p and δm_d are denoted for infinitesimal variations in applied moments onto the MP and $\mathscr{D}_p$ about $\mathbf{z}_b$. o_p and o_d correspond to the infinitesimal changes in rotation of the MP and drum about $\mathbf{z}_b$.

Hereafter, we investigate the stiffness of a CDPR with linear cable model. The elastic behavior of the MP is described as follows:

$$\mathbf{K} = \frac{d\mathbf{w}_e}{d\mathbf{r}} \tag{15}$$

The following equation is achieved by substituting Eq. (10) into Eq. (15) [2].

$$\mathbf{K} = -\frac{d\mathbf{W}\mathbf{t}}{d\mathbf{r}} = \mathbf{K}_a + \mathbf{K}_p = -\frac{d\mathbf{W}}{d\mathbf{r}}\mathbf{t} - \mathbf{W}\frac{d\mathbf{t}}{d\mathbf{r}} \tag{16}$$

Passive stiffness matrix, $\mathbf{K}_p$, depends on the cable properties and active stiffness matrix, $\mathbf{K}_a$, depends on the cable tension, $\mathbf{t}$.

Passive stiffness matrix Under the assumption of the linear spring model for cables, the following equation represents the cable elasticity, where i-th cable elasticity coefficient and length variations are denoted as k_i and δl_i, respectively.

$$t_i = k_i \delta l_i \tag{17}$$

Equation (17) is rewritten for all the cables in the following closed form.

$$\mathbf{t} = \mathbf{K}_l \delta\mathbf{l} \tag{18}$$

where, $\delta\mathbf{l} = [\delta l_1, \delta l_2, \delta l_3]^T$ is the vector of infinitesimal variation in cable length and the general stiffness cables-stiffness matrix,

$\mathbf{K}_l$ is defined as follows:

$$\mathbf{K}_l = \begin{bmatrix} k_1 & 0 & 0 \\ 0 & k_2 & 0 \\ 0 & 0 & k_3 \end{bmatrix} \tag{19}$$

The wrench matrix,$\mathbf{W}$ is defined as

$$\mathbf{W}^T = -\frac{\mathrm{d}\mathbf{l}}{\mathrm{d}\mathbf{r}} \tag{20}$$

Where, $\mathbf{l} = [l_1, l_2, l_3]^T$ is cable length vector. From Eq. (18) and Eq. (20) we rewrite the passive stiffness matrix as:

$$\mathbf{K}_p = -\mathbf{W}\mathbf{K}\frac{\mathrm{d}\mathbf{l}}{\mathrm{d}\mathbf{r}} = \mathbf{W}\mathbf{K}_l\mathbf{W}^T \tag{21}$$

By substituting Eq. (11) and Eq. (19) into Eq. (21) we can formulate passive stiffness matrix as follows:

$$\mathbf{K}_p = \sum_{i=1}^{3} k_i \begin{bmatrix} {}^b\mathbf{u}_i {}^b\mathbf{u}_i{}^T & {}^b\mathbf{u}_i {}^b\mathbf{u}_i{}^T \mathbf{E}^r\mathbf{b}_i & w_{3,i}\,{}^b\mathbf{u}_i \\ {}^r\mathbf{b}_i{}^T\mathbf{E}^{T\,b}\mathbf{u}_i {}^b\mathbf{u}_i{}^T & {}^r\mathbf{b}_i{}^T\mathbf{E}^{T\,b}\mathbf{u}_i {}^b\mathbf{u}_i{}^T\mathbf{E}^r\mathbf{b}_i & w_{3,i}\,{}^r\mathbf{b}_i{}^T\mathbf{E}^{T\,b}\mathbf{u}_i \\ w_{3,i}\,{}^b\mathbf{u}_i{}^T & w_{3,i}\,{}^b\mathbf{u}_i{}^T\mathbf{E}^r\mathbf{b}_i & w_{3,i}{}^2 \end{bmatrix} \tag{22}$$

where, ${}^r\mathbf{b}_i = {}^b\mathbf{R}_p{}^p\mathbf{b}_i$ and $w_{3,i}$ refers to the third row and the ith column of $\mathbf{W}$.

Active stiffness matrix From Eq. (16) the active stiffness matrix can be rewritten as follows:

$$\mathbf{K}_a = -\frac{\mathrm{d}\mathbf{W}}{\mathrm{d}\mathbf{r}}\mathbf{t} = -\sum_{i=1}^{3}\frac{\mathrm{d}\mathbf{w}_i}{\mathrm{d}\mathbf{r}}t_i \tag{23}$$

where the differential of wrench matrix associated to ith cable with respect to the infinitesimal screw, $\delta\mathbf{r}$ is given by:

$$\frac{\mathrm{d}\mathbf{w}_i}{\mathrm{d}\mathbf{r}} = \begin{bmatrix} \frac{\mathrm{d}^b\mathbf{u}_i}{\mathrm{d}\mathbf{p}} & \frac{\mathrm{d}^b\mathbf{u}_i}{\mathrm{d}o_p} & \frac{\mathrm{d}^b\mathbf{u}_i}{\mathrm{d}o_d} \\ \frac{\mathrm{d}\left({}^r\mathbf{b}_i{}^T\mathbf{E}^{T\,b}\mathbf{u}_i\right)}{\mathrm{d}\mathbf{p}} & \frac{\mathrm{d}\left({}^r\mathbf{b}_i{}^T\mathbf{E}^{T\,b}\mathbf{u}_i\right)}{\mathrm{d}o_p} & \frac{\mathrm{d}\left({}^r\mathbf{b}_i{}^T\mathbf{E}^{T\,b}\mathbf{u}_i\right)}{\mathrm{d}o_d} \\ \frac{\mathrm{d}w_{3,i}}{\mathrm{d}\mathbf{p}} & \frac{\mathrm{d}w_{3,i}}{\mathrm{d}o_p} & \frac{\mathrm{d}w_{3,i}}{\mathrm{d}o_d} \end{bmatrix} \tag{24}$$

The differential form of ${}^b\mathbf{u}_i$ is derived from Eq. (1) in the following

$$\mathrm{d}^b\mathbf{u}_i = -\frac{1}{l_i}(\mathbf{I}_{2,2} - {}^b\mathbf{u}_i{}^b\mathbf{u}_i{}^T)(\mathrm{d}\mathbf{p} - {}^b\mathbf{R}_p\mathbf{E}^p\mathbf{b}_i\mathrm{d}o_p) \tag{25}$$

and the differential term in the second row of Eq. (24) is determined as follows:

$$\mathrm{d}\left({}^r\mathbf{b}_i{}^T\mathbf{E}^{T\,b}\mathbf{u}_i\right) = -{}^p\mathbf{b}_i^T{}^b\mathbf{R}_p{}^b\mathbf{u}_i + {}^r\mathbf{b}_i{}^T\mathbf{E}^T\mathrm{d}^b\mathbf{u}_i \tag{26}$$

Therefore, The active stiffness matrix of the CDPC is reformulated in Eq. (27).

$$\mathbf{K}_a = -\sum_{i=1}^{m} t_i \begin{bmatrix} \frac{\mathrm{d}^b\mathbf{u}_i}{\mathrm{d}\mathbf{p}} & \frac{\mathrm{d}^b\mathbf{u}_i}{\mathrm{d}o_p} & \frac{\mathrm{d}^b\mathbf{u}_i}{\mathrm{d}o_d} \\ \frac{\mathrm{d}\left({}^r\mathbf{b}_i{}^T\mathbf{E}^{T\,b}\mathbf{u}_i\right)}{\mathrm{d}\mathbf{p}} & \frac{\mathrm{d}\left({}^r\mathbf{b}_i{}^T\mathbf{E}^{T\,b}\mathbf{u}_i\right)}{\mathrm{d}o_p} & \frac{\mathrm{d}\left({}^r\mathbf{b}_i{}^T\mathbf{E}^{T\,b}\mathbf{u}_i\right)}{\mathrm{d}o_d} \\ \frac{\mathrm{d}w_{3,i}}{\mathrm{d}\mathbf{p}} & \frac{\mathrm{d}w_{3,i}}{\mathrm{d}o_p} & \frac{\mathrm{d}w_{3,i}}{\mathrm{d}o_d} \end{bmatrix} \tag{27}$$

where,

$$\frac{\mathrm{d}^b\mathbf{u}_i}{\mathrm{d}\mathbf{p}} = -\frac{1}{l_i}(\mathbf{I}_{2,2} - {}^b\mathbf{u}_i{}^b\mathbf{u}_i{}^T) \tag{28}$$

$$\frac{\mathrm{d}^b\mathbf{u}_i}{\mathrm{d}o_p} = \frac{1}{l_i}(\mathbf{I}_{2,2} - {}^b\mathbf{u}_i{}^b\mathbf{u}_i{}^T){}^b\mathbf{R}_p\mathbf{E}^p\mathbf{b}_i \tag{29}$$

$$\frac{\mathrm{d}^b\mathbf{u}_i}{\mathrm{d}o_d} = \mathbf{0}_{2,1} \tag{30}$$

$$\frac{\mathrm{d}\left({}^r\mathbf{b}_i{}^T\mathbf{E}^{T\,b}\mathbf{u}_i\right)}{\mathrm{d}\mathbf{p}} = -\frac{1}{l_i}{}^r\mathbf{b}_i^T\mathbf{E}^T(\mathbf{I}_{2,2} - {}^b\mathbf{u}_i{}^b\mathbf{u}_i{}^T) \tag{31}$$

$$\frac{\mathrm{d}\left({}^r\mathbf{b}_i{}^T\mathbf{E}^{T\,b}\mathbf{u}_i\right)}{\mathrm{d}o_p} = \frac{1}{l_i}{}^r\mathbf{b}_i^T\mathbf{E}^T(\mathbf{I}_{2,2} - {}^b\mathbf{u}_i{}^b\mathbf{u}_i{}^T){}^b\mathbf{R}_p\mathbf{E}^p\mathbf{b}_i - {}^p\mathbf{b}_i^T{}^b\mathbf{R}_p{}^b\mathbf{u}_i \tag{32}$$

$$\frac{\mathrm{d}\left({}^r\mathbf{b}_i{}^T\mathbf{E}^{T\,b}\mathbf{u}_i\right)}{\mathrm{d}o_d} = 0 \tag{33}$$

$$\frac{\mathrm{d}w_{3,i}}{\mathrm{d}\mathbf{p}} = \mathbf{0}_{1,2} \tag{34}$$

$$\frac{\mathrm{d}w_{3,i}}{\mathrm{d}o_p} = 0 \tag{35}$$

$$\frac{\mathrm{d}w_{3,i}}{\mathrm{d}o_d} = 0 \tag{36}$$

The static model presented in this section is required for further investigation regarding static workspace, required height of the CDPC and positioning of the payload.

4 REQUIRED HEIGHT FOR A GIVEN PAYLOAD

In this section, we study the minimum required height of the CDPC for manipulating a given payload. In general, suspended CDPRs are incapable of performing tasks close to their exit points i.e., the larger part of their workspace is usually closer

to the ground for a given external wrench. Here, we elaborate a method that approximates the required height of the CDPC for lifting a given payload within its workspace.

If the input torques to the two ends of the cable loop ($\mathscr{C}_1$, $\mathscr{C}_2$) are equal, then it will behave as a single cable, $\mathscr{C}_{12}$, connecting points A_{12} to B_{12} as depicted in Fig. 3. For this model, the MP is assumed to have a constant orientation ($\theta = 0$) within its workspace.

The static workspace of the CDPC is defined as the set of all the points of MP namely, point P whose cable tensions belong to the specified cable limits for respecting the static equilibrium of the CDPC. Equation (37) formulates the static equilibrium.

$$WS = \{(x,\, y) \in \mathbb{R}^2,\ \exists\, t_m \in [t_{min},\ t_{max}] \text{ s.t. } \mathbf{W}_m \mathbf{t}_m + m\mathbf{g} = \mathbf{0}_{2,1}\} \tag{37}$$

where, minimum and maximum cable tensions are denoted as t_{min} and t_{max}, respectively. and the tension vector associated to the described model of CDPC with two cables is given by

$$\mathbf{t}_m = \begin{bmatrix} t_{12} & t_3 \end{bmatrix}^T \tag{38}$$

$\mathbf{W}_m$ is the wrench matrix of the considered model and is expressed as follows:

$$\mathbf{W}_m = \begin{bmatrix} {}^b\mathbf{u}_{12} & {}^b\mathbf{u}_3 \end{bmatrix} \tag{39}$$

From Eqs. (37-39) the equilibrium of the external forces applied onto the MP is reformulated as follows:

$$t_{12}\,{}^b\mathbf{u}_{12} + t_3\,{}^b\mathbf{u}_3 + m\mathbf{g} = \mathbf{0}_{2,1} \tag{40}$$

Let us compute $\mathbf{v}_{12}$ and $\mathbf{v}_3$, the unit vector orthogonal to ${}^b\mathbf{u}_{12}$ and ${}^b\mathbf{u}_{12}$, respectively.

$$\mathbf{v}_i = \mathbf{E}\,{}^b\mathbf{u}_i, \quad i = (12),\, 3 \tag{41}$$

with

$$\mathbf{E} = \begin{bmatrix} 0 & -1 \\ 1 & 0 \end{bmatrix} \tag{42}$$

The following equation is derived from Eq. (40) by replacing t_{12} with $2t_{max}$, and eliminating t_3 by a dot product.

$$\mathbf{v}_3^T \left(2t_{max}\,{}^b\mathbf{u}_{12} + t_3\,{}^b\mathbf{u}_3 + m\mathbf{g}\right) = 0 \tag{43}$$

similarly, the following equation is obtained by replacing t_3 with t_{max} and eliminating t_1.

$$\mathbf{v}_{12}^T \left(t_{12}\,{}^b\mathbf{u}_{12} + t_{max}\,{}^b\mathbf{u}_3 + m\mathbf{g}\right) = 0 \tag{44}$$

Hereafter, by solving Eqs. (43) and (44) for p_y we obtain the following equation

$$y_i = \zeta_i\, mg \left(l_b l_p - \frac{1}{2}l_p^2 + 2x^2 - \frac{1}{2}l_b^2\right) + h_b \quad i = (12),\, 3 \tag{45}$$

where, y_{12} and y_3 stand for the y_p loci whose associated cable tension is considered as the maximum allowed tension for cables $\mathscr{C}_{12}$ and $\mathscr{C}_3$, respectively. ζ_{12} and ζ_3 are defined as:

$$\zeta_{12} = \frac{1}{\sqrt{16\, t_{max}^2 (l_b - l_p)^2 - m^2 g^2 (l_b - l_p - 2x)^2}} \tag{46}$$

$$\zeta_3 = \frac{1}{\sqrt{4\, t_{max}^2 (l_b - l_p)^2 - m^2 g^2 (l_b - l_p + 2x)^2}} \tag{47}$$

Equations (46) and (47) imply the validity domain of Eq. (45) as formulated in the following equations.

$$x_{lb,12} = \frac{(l_b - l_p)(mg - 4t_{max})}{2mg} \tag{48}$$

$$x_{ub,12} = \frac{(l_b - l_p)(mg + 4t_{max})}{2mg} \tag{49}$$

The valid domain for y_3 is expressed in the following equations:

$$x_{lb,3} = \frac{(l_p - l_b)(mg + 2t_{max})}{2mg} \tag{50}$$

$$x_{ub,3} = \frac{(l_p - l_b)(mg - 2t_{max})}{2mg} \tag{51}$$

Therefore, the domain, $\mathbf{x}_i = [x_{lb,i},\, x_{ub,i}],\ \ i = (12),\, 3$, is defined for the boundary equations, y_i. From Eq. (45) we state that, there is always a minimum point on the upper-boundary equations namely, $\mathbf{m}_i = [\underline{x_i}, \underline{y_i}]^T,\ \ i = (12),\, 3$. The latter point is associated to the minimum of the upper-boundary equations and satisfies the following equation.

$$\frac{\mathrm{d}\, y_i(\underline{x_i})}{\mathrm{d}\, x} = 0 \qquad i = (12),\, 3 \tag{52}$$

Hereafter, we define the maximum required height of the payload as h_l, and the minimum required height of the building

as follows:

$$h_b = h_c + \bar{h}_l \tag{53}$$

In order to calculate the minimum required height for the ceiling, we define h_c in Eq. (54). The latter parameter is associated to the minimum required distance from ceiling that the MP can support the given payload within the boundary of the cable tensions. It should be noted that, h_c depends on the maximum cable tension, weight and the length of the frame and MP.

$$h_c = h_b - \bar{y}_p \tag{54}$$

We define $\bar{y}_p$ as the maximum value of y_p that the MP could obtain for any $p_x \in \left[\frac{l_p - l_b}{2}, \frac{l_b - l_p}{2}\right]$. The following equation yields $\bar{y}_p$:

$$\bar{y}_p = \min(\underline{y}_{12}, \underline{y}_3) \tag{55}$$

In the previous equation, $\underline{y}_{12}$ and $\underline{y}_3$ state the minimum values of y_{12} and y_3, respectively.

Figure 4 shows the workspace of CDPC, the upper-boundaries and h_c for different masses and heights of the ceiling. Maximum cable tension (t_{max} =220 N), height of the MP (h_p=0.5 m) and the length of the CDPC frame (l_b=0.5 m) are constant.

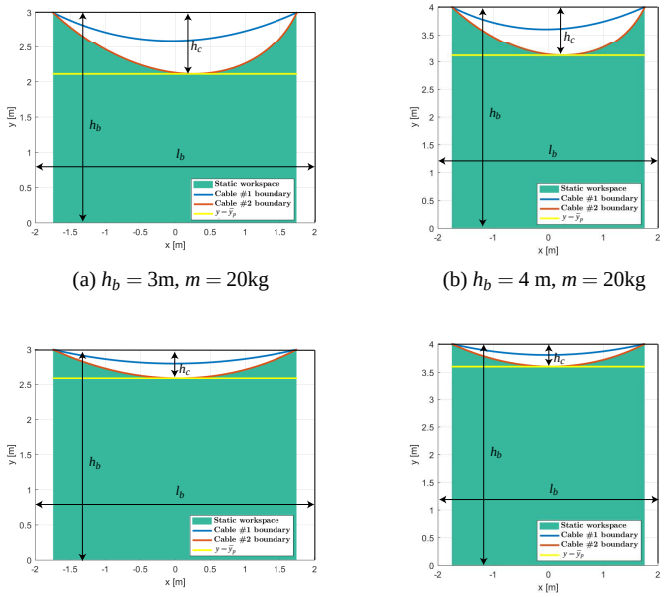

(a) $h_b = 3$m, $m = 20$kg (b) $h_b = 4$ m, $m = 20$kg

(c) $h_b = 3$m, $m = 10$kg (d) $h_b = 4$ m, $m = 10$kg

Figure 4: Workspace of CDPC for different heights and the overall mass (MP and payload)

5 THE EFFECTS OF THE HOISTING TORQUE ON THE POSITIONING

The design of the CDPC and its applications are discussed in the previous sections. Nevertheless, the effects of the hoisting torque or more precisely, the torque generated by a cable loop on the kinematic has not been addressed. In [3], The impact of using a cable loop for articulating a MP of a CDPR is studied. Here, the parasitic inclinations of the MP are defined as a function of the moment induced by the cable loop and the MP pose. Parasitic inclinations deal with the inclination of the MP and as a consequence the positioning error of the payload.

Determining inclination of the moving-platform

This approach takes into account only the equilibrium of the moments applied/sustained about Instantaneous Center of Rotation (ICR) point regardless of the cables tension (t_1, t_2, t_3), but the difference of cable loop tensions, namely, δt. The following equation expresses the equilibrium of the moments applied/sustained about ICR, point I, expressed in $\mathscr{F}_b$.

$$m_{12} + m_w = 0 \tag{56}$$

m_{12} is the moment applied onto the MP at point I due to cable tension difference δt. Then, moment m_{12} can be expressed as follows:

$$m_{12} = r_p \delta t \tag{57}$$

m_w is the moment applied onto the MP expressed at point I due to the MP weight, which is passing through point C.

$$m_w = ({}^b\mathbf{c} - {}^b\mathbf{i})^T \mathbf{E}^T m\mathbf{g} \tag{58}$$

under the assumption that segments A_1B_1 and A_2B_2 are parallel, which is valid as long as the MP is far from the points A_1 and A_2. In this approach the Cartesian coordinate vector of point I, ${}^b\mathbf{i}$, is computed to formulate the pure rotation of the MP about this point.

ICR is the intersection point between the line $\mathscr{L}_{12}$ passing

through points A_{12} and B_{12} and the line $\mathscr{L}_3$ passing through points A_3 and B_3. The equations of lines $\mathscr{L}_{12}$ and $\mathscr{L}_3$ are expressed as:

$$\mathscr{L}_{12}: \; x(b_{12y}-a_{12y})+y(a_{12x}-b_{12x})-a_{12x}b_{12y}+a_{12y}b_{12x}=0 \tag{59}$$

$$\mathscr{L}_3: \; x(b_{3y}-a_{3y})+y(a_{3x}-b_{3x})-a_{3x}b_{3y}+a_{3y}b_{3x}=0 \tag{60}$$

The Cartesian coordinate vector of points A_{12} and B_{12}, namely, ${}^b\mathbf{a}_{12}=[a_{12x},\, a_{12y}]^T$ and ${}^b\mathbf{b}_{12}=[b_{12x},\, b_{12y}]^T$ are the followings:

$${}^b\mathbf{a}_{12}=\frac{1}{2}({}^b\mathbf{a}_1+{}^b\mathbf{a}_2) \tag{61}$$

$${}^b\mathbf{b}_{12}=\frac{1}{2}({}^b\mathbf{b}_1+{}^b\mathbf{b}_2)={}^b\mathbf{p}+\frac{1}{2}{}^b\mathbf{R}_p({}^p\mathbf{b}_1+{}^p\mathbf{b}_2) \tag{62}$$

I being the intersection point of lines $\mathscr{L}_{12}$ and $\mathscr{L}_3$, and of Cartesian coordinate vector, ${}^b\mathbf{i}\equiv\mathscr{L}_{12}\cap\mathscr{L}_3$:

$${}^b\mathbf{i}=[i_x,\, i_y]^T \tag{63}$$

with i_x and i_y being expressed as:

$$i_x=\frac{\mu_1\nu_2-\mu_2\nu_1}{\lambda_1\mu_2-\lambda_2\mu_1},\quad i_y=\frac{-\nu_1-\lambda_1 i_x}{\mu_1} \tag{64}$$

with

$$\begin{aligned}
\lambda_1 &= \frac{1}{2}c_\theta(b_{1y}+b_{2y})+\frac{1}{2}s_\theta(b_{1x}+b_{2x})-\frac{1}{2}(a_{1y}-a_{2y})+p_y\\
\lambda_2 &= b_{3x}s_\theta+b_{3y}-a_{3y}c_\theta-a_{3y}+p_y\\
\mu_1 &= -\frac{1}{2}c_\theta(b_{1x}+b_{2x})+\frac{1}{2}s_\theta(b_{1y}+b_{2y})+\frac{1}{2}(a_{1x}+a_{2x})-p_x\\
\mu_2 &= b_{3y}s_\theta-b_{3x}c_\theta+a_{3x}-p_x\\
\nu_1 &= \frac{1}{4}c_\theta[(-a_{1x}-a_{2x})(b_{1y}+b_{2y})+(b_{1x}+b_{2x})(a_{1y}+a_{2y})]\\
&\quad+\frac{1}{4}s_\theta[(-a_{1x}-a_{2x})(b_{1x}+b_{2x})-(b_{1y}+b_{2y})(a_{1y}+a_{2y})]\\
&\quad-\frac{1}{2}p_y(a_{1x}-a_{2x})+\frac{1}{2}p_x(a_{1y}-a_{2y})\\
\nu_2 &= (a_{3y}b_{3x}-a_{3x}b_{3y})c_\theta-(a_{3x}b_{3x}+a_{3y}b_{3y})s_\theta-a_{3x}p_y+a_{3y}p_x
\end{aligned} \tag{65}$$

In Fig. 3, all the relevant notations are illustrated. ICR point, I, is a function of θ, ${}^b\mathbf{p}$, ${}^b\mathbf{a}_i$ and ${}^p\mathbf{b}_i$, $i=1,\,2,\,3$.

By using the following tangent half-angle substitution in Eq. (66), Eq. (56) becomes the $6th$ order univariate polynomial equation (68).

$$\sin\theta=\frac{2t_\theta}{1+t_\theta^2},\quad \cos\theta=\frac{1-t_\theta^2}{1+t_\theta^2} \tag{66}$$

and,

$$t_\theta=\tan\frac{\theta}{2} \tag{67}$$

From Eqs. (63)-(67) we can rewrite Eq. (56) as follows:

$$C_6{t_\theta}^6+C_5{t_\theta}^5+C_4{t_\theta}^4+C_3{t_\theta}^3+C_2{t_\theta}^2+C_1t_\theta+C_0=0 \tag{68}$$

Equation (68) is a function of t_θ. The obtained polynomial is solved numerically to find t_θ. Then, θ can be substituted with t_θ based on Eq. (67). The coefficients of the latter polynomial, $C_0, C_1, ..., C_6$, are detailed in [2]. Equation (68) is solved in order to find the possible inclination(s) θ of the MP for a given position of its geometric center P.

Parasitic inclination, θ_p, is defined as undesired orientation of the MP that leads to inaccuracy in manipulation and positioning. This kinematic situation is an outcome of utilizing cable loop in the CDPR. Since parasitic inclination decreases the accuracy of the robot, its investigation is crucial and can be employed to minimize the parasitic inclination by optimizing the design parameters in the design stage. The following steps are carried out to determine θ_p of the MP due to cable tension differences, δt, into the cable-loop.

1. To determine the natural inclination θ_n of the MP. θ_n amounts to the rotation angle θ of the MP for the same tensions in both strands $\mathscr{C}_1$ and $\mathscr{C}_2$ of the cable-loop, i.e., $\delta t=0$.
2. To determine the inclination θ_m of the moving-platform when tensions in both strands of the cable-loop are not the same, i.e., $\delta t\neq 0$.

Position of the end-effector and hoistig torque

In order to perform the pick and place task, position of the end-effector should be computed. As the hoisting torque, m_{12}, effects on the overall inclination of the MP and consequently the position of the end-effector, we calculate the end-effector position namely, ${}^b\mathbf{e}$, for the following two cases:

[2] https://drive.google.com/file/d/0B80GqJ5822jObDlXNkdOUWd6UUE/view?usp=sharing

1. When no hoisting torque is applied to the hoist, i.e., $m_{12} = 0$.

$$^{b}\mathbf{e}_n = {}^{b}\mathbf{h}_n + \begin{bmatrix} 0 \\ -h_l \end{bmatrix} \tag{69}$$

where, $^{b}\mathbf{e}_n$ stands for the Cartesian coordinate vector of end-effector (point E as shown in Fig. 3) without hoisting torque. The corresponding Cartesian coordinate vector of point H is formulated as follows.

$$^{b}\mathbf{h}_n = {}^{b}\mathbf{p} + {}^{b}\mathbf{R}_p(\theta_n)\,{}^{p}\mathbf{h} \tag{70}$$

and the position of the hoist anchor point expressed in $\mathscr{F}_p$ namely, $^{p}\mathbf{h}$ is determined as detailed in the following.

$$^{p}\mathbf{h} = {}^{p}\mathbf{c} + [r_h,\ -(r_{g1} + r_{g2})]^T \tag{71}$$

where, r_{g1} stands for the radius of the gear attached to the shaft $\mathscr{S}_1$, r_{g2} is the radius of the green gear attached to the shaft $\mathscr{S}_2$ and r_h is the radius of $\mathscr{D}_h$.

2. The position of the hoist anchor point when $m_{12} \neq 0$ is expressed in the following equation.

$$^{b}\mathbf{e}_m = {}^{b}\mathbf{h}_m + \begin{bmatrix} 0 \\ -h_l \end{bmatrix} \tag{72}$$

where,

$$^{b}\mathbf{h}_m = {}^{b}\mathbf{p} + {}^{b}\mathbf{R}_p(\theta_m)\,{}^{p}\mathbf{h} \tag{73}$$

Therefore, the position of the end-effector is obtained for unactuated hoist as $^{b}\mathbf{e}_n$, while the parasitic inclination due to actuated hoist varies the position of the end-effector to $^{b}\mathbf{e}_m$.

6 CONCLUSIONS

This paper introduced a new conceptual design of cable-driven parallel robot connected to a hoist mechanism for lifting payloads. The robot exploits cables to transmit power directly from fixed motors to the moving-platform. In comparison with conventional cable-driven parallel robots and cable-driven suspended robots, the proposed concept is less at risk of interfering with objects within the workspace, as the moving platform can remain higher above the ground. The proposed cable-driven cranes are inexpensive and could be an interesting alternative to bridge-crane mechanisms. The architecture and static model of the robot were detailed in this paper. The static workspace and maximum required height for the robot were investigated. The effect of hoisting torque on the moving-platform inclination was also investigated. It was shown that the angle of inclination can be computed efficiently and reliably. The detailed design and the prototyping of the cable-driven parallel crane are left for future work.

REFERENCES

[1] Gagliardini, L., Caro, S., Gouttefarde, M., and Girin, A., 2016. "Discrete reconfiguration planning for cable-driven parallel robots". *Mechanism and Machine Theory*, ***100***, pp. 313–337.

[2] Gagliardini, L., 2016. "Discrete reconfigurations of cable-driven parallel robots". PhD thesis, Ecole Centrale de Nantes (ECN).

[3] Lessanibahri, S., Cardou, P., and Caro, S., 2018. "Parasitic inclinations in cable-driven parallel robots using cable loops". *Procedia CIRP*, ***70***, pp. 296–301.

[4] Gouttefarde, M., Collard, J.-F., Riehl, N., and Baradat, C., 2012. "Simplified static analysis of large-dimension parallel cable-driven robots". In Robotics and Automation (ICRA), 2012 IEEE International Conference on, IEEE, pp. 2299–2305.

[5] Riehl, N., Gouttefarde, M., Krut, S., Baradat, C., and Pierrot, F., 2009. "Effects of non-negligible cable mass on the static behavior of large workspace cable-driven parallel mechanisms". In Robotics and Automation, 2009. ICRA'09. IEEE International Conference on, IEEE, pp. 2193–2198.

[6] Gosselin, C., 1990. "Stiffness mapping for parallel manipulators". *IEEE Transactions on Robotics and Automation*, ***6***(3), pp. 377–382.

[7] Merlet, J.-P., 2006. *Parallel robots*, Vol. 128. Springer Science & Business Media.

[8] Yuan, H., 2015. "Static and dynamic stiffness analysis of cable-driven parallel robots". PhD thesis, INSA de Rennes.

[9] Behzadipour, S., and Khajepour, A., 2006. "Stiffness of cable-based parallel manipulators with application to stability analysis". *Journal of mechanical design*, ***128***(1), pp. 303–310.

[10] Carricato, M., 2013. "Inverse geometrico-static problem of underconstrained cable-driven parallel robots with three cables". *Journal of Mechanisms and Robotics*, ***5***(3), p. 031002.

[11] Platis, A., Rasheed, T., Cardou, P., and Caro, S., 2018. "Isotropic design of the spherical wrist of a cable-driven parallel robot". In *Advances in Robot Kinematics 2016*. Springer, pp. 321–330.

[12] Nagai, K., Le, T. N., Hayashi, Y., and Ito, K., 2012. "Kinematical analysis of redundant drive wire mechanisms with velocity constraint". In Mechatronics and Automa-

tion (ICMA), 2012 International Conference on, IEEE, pp. 1496–1501.

[13] Lin, R., Guo, W., and Gao, F., 2016. "On parasitic motion of parallel mechanisms". In ASME 2016 International Design Engineering Technical Conferences and Computers and Information in Engineering Conference, American Society of Mechanical Engineers, pp. V05BT07A077–V05BT07A077.

[14] Le, T. N., Dobashi, H., and Nagai, K., 2016. "Kinematical and static force analysis on redundant drive wire mechanism with velocity constraint modules to reduce the number of actuators". *ROBOMECH Journal*, ***3***(1), p. 22.